Coherent control of electron spin dynamics in nano-engineered semiconductor structures

Denega, Sergii Zinoviyovych

Chapter 3

Suppressed spin dephasing for 2D and bulk electrons in GaAs wires due to engineered cancellation of spin-orbit interaction terms

Abstract

We report a study of suppressed spin dephasing for quasi-one-dimensional electron ensembles in wires etched into a GaAs/AlGaAs heterojunction system. Time-resolved Kerr-rotation measurements show a suppression that is most pronounced for wires along the [110] crystal direction. This is the fingerprint of a suppression that is enhanced due to a strong anisotropy in spin-orbit fields that can occur when the Rashba and Dresselhaus contributions are engineered to cancel each other. A surprising observation is that this mechanisms for suppressing spin dephasing is not only effective for electrons in the heterojunction quantum well, but also for electrons in a deeper bulk layer.

This chapter is based on Ref. 4 on p. 103.

3.1 Introduction

For electron ensembles in semiconductor device structures the dominant mechanism for spin dephasing and spin relaxation is often due to spin-orbit interaction (SOI). A current challenge in the field of spintronics is therefore to obtain control over such relaxation, or to even turn SOI into a resource for spin manipulation [1]. GaAs/AlGaAs based heterostructures provide here an interesting platform. Besides high material quality and good optical selection rules, these materials can be engineered to have two types of SOI: Dresselhaus SOI, resulting from lack of inversion symmetry in the GaAs crystal structure, and Rashba SOI, effective when electrons are confined in a layer with bending of the conduction band [2]. Such SOI acts as a k-vector-dependent effective magnetic field on electron spins. Notably, the strength of these two effects can be tuned to exactly cancel each other [3, 4] for electrons with the k vector in [110] direction [Fig. 3.1(a)]. This notion is central in many proposals [5, 7, 6, 8, 9] that aim at suppressing spin relaxation effects. Work on unpatterned quantum-well areas with techniques that filter out signals from electrons with [110] k vectors confirmed reduced dephasing for these electrons [10, 11, 4].

We report here the observation that this cancellation of two SOI terms can directly result in suppressed spin dephasing for an entire electron ensemble in a wire along the [110] direction. Notably, this does not require that full quantum confinement restricts electron transport in the wire to the [110] direction. Instead, it concerns a strong enhancement of a motional-narrowing type effect that results from frequent scattering on the boundaries of quasi-one-dimensional (1D) wires [12, 13, 14] that can—with further tuning—suppress spin dephasing by several orders of magnitude [15, 16]. Quasi-1D systems are here defined as having the wire width too wide for 1D quantum confinement, but smaller than the spin precession length (ballistic travel distance during which spins precess an angle π in the sum of spin-orbit fields and external magnetic field). In addition, the wire width should not be much in excess of the mean free path.

3.2 Experimental realization

We used electron ensembles in GaAs/AlGaAs wires (Fig. 3.1) that contain a heterojunction-based two-dimensional electron gas (2DEG) for which the Rashba and linear Dresselhaus SOI are of similar strength [3]. We used time-resolved Kerr readout for directly testing whether quasi-1D confinement in device structures

combined with anisotropy for SOI in k space can be tuned to give a pronounced suppression for spin dephasing for wires in the [110] direction. For 2DEG electrons we indeed observe this behavior, which we will further call spin-dephasing anisotropy (SDA). Surprisingly, we also obtained evidence for a new manifestation of SDA: a contribution to our Kerr signals from a deeper bulk layer in our wires also shows SDA. We can explain these observations by considering that an electron ensemble in a bulk layer with weak band bending [Fig. 3.1(c)] is also subject to a Rashba-type SOI and we find agreement with numerical modeling of such a situation.

We fabricated arrays of quasi-1D wires with electron-beam lithography and subsequent wet etching of a GaAs/AlGaAs heterojunction system with a 2DEG at 114 nm depth (etch depth ∼100 nm). Figure 3.1(b) is a micrograph of an array with wires along [110] (1.2 μm wire width and 1.6 μm periodicity). Other

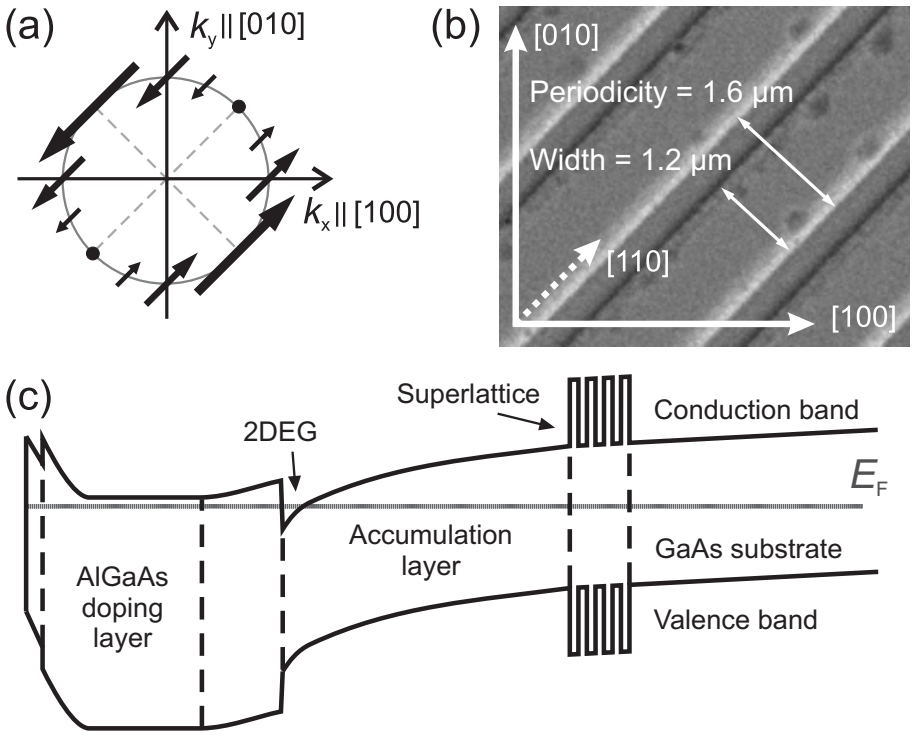

Figure 3.1: (a) Dependence of spin-orbit fields on k vector on the Fermi circle in the k_x-k_y plane for equal strength of Rashba and linear Dresselhaus effect. (b) Scanning-electron micrograph for a section of a wire array oriented along the [110] crystal direction. (c) Band diagram of the GaAs/AlGaAs heterostructure (not to scale), with a 2DEG where the conduction band bends below the Fermi energy E_F.

areas had [100], [010], and [-110] oriented wires, and for reference we had both unpatterned and fully etched areas. Figure 3.1(c) shows a band diagram of the GaAs/AlGaAs heterostructure along growth direction. The layer sequence starts with an intrinsic (001) oriented GaAs substrate, followed by a training layer (superlattice with 10 periods of 5.2 nm GaAs and 10.6 nm AlAs). Then a 933 nm undoped GaAs accumulation layer is followed by a 37 nm undoped $Al_{0.32}Ga_{0.68}As$ spacer layer. On top of this 72 nm homogeneously Si-doped $Al_{0.32}Ga_{0.68}As$ is grown. The heterostructure is finished by a 5 nm GaAs cap layer. The 2DEG is at the heterojunction between the AlGaAs spacer layer and the GaAs accumulation layer. Under illuminated conditions at 4.2 K the electron density is $n_{2D} = 4.7 \times 10^{15}$ m^{-2} and the mean free path is $\sim$30 μm.

The spin dynamics was probed with conventional [17] mono-color time-resolved Kerr-rotation measurements in an optical cryostat at 4.2 K with magnetic fields (magnitude B) up to 7 T. We used a tunable Ti:sapphire laser with $\sim$150 fs pulses at 80 MHz repetition rate. The spectrum of pulses was wider than Fourier-transform limited, with significant amplitudes over a $\sim$15 meV window. Samples were excited at normal incidence with a circularly polarized pump pulse (helicity modulated at 50 kHz with a photoelastic modulator for avoiding nuclear polarization). This induces a nonequilibrium electron ensemble in the conduction band with a net spin orientation along the growth direction of the sample. The evolution of the spin ensemble is recorded by measuring the 50 kHz component in Kerr rotation after reflection of a linearly polarized probe pulse with a polarization bridge, as a function of pump-probe delay t. We used spot diameters of about 100 μm on wire arrays of larger dimensions [18]. All data were taken at pump-photon density $n_{ex} \approx 3{\times}10^{15}$ m^{-2} per pulse. Measurements were performed with the external field in [110] direction, unless stated otherwise.

3.3 Signatures of spin dephasing anisotropy for 2DEG and bulk electrons

While a heterojunction system is for our research an interesting material given the strong and tunable band bending in the 2DEG layer, it imposes difficulties for an experiment with optical probing (as compared to double sided quantum wells). The bandgaps for the 2DEG layer, and deeper parts of the accumulation layer and the substrate are nearly identical [Fig. 3.1(c)], so probing must use reflection and one cannot avoid that Kerr signals have contributions from both 2DEG electrons

and bulk electrons in these deeper layers. We recently characterized [19] that it is for our material nevertheless possible to isolate the Kerr signal from 2DEG electrons when pumping at least ∼20 meV above the bottom of the conduction band for bulk (we used 1.55 eV). In summary, at pump intensities with $n_{ex} \leq n_{2D}$ the Kerr signal θ_K is a superposition of two mono-exponentially decaying cosines,

$$\theta_K = \sum_{i=1,2} A_i \exp\left(-\frac{t}{\tau_i}\right) \cos\left(\frac{|g_i|\mu_B B}{\hbar} t + \phi_i\right) \tag{3.1}$$

with amplitudes A_i, g factors $|g_i|$, dephasing times τ_i, and ϕ_i are apparent initial phases [20] for spin precession. This also applies to the data that we present here. Figures 3.2(a) and 3.3(a) show Kerr signals from wires, recorded in fields of 0 T to 7 T. In particular at high fields, the envelopes of oscillating Kerr signals show clear nodes and anti-nodes and we checked that all Fourier transforms of data taken at $B > 3$ T showed two pronounced peaks at g factors $|g_1| \approx 0.36$ and $|g_2| \approx 0.43$. Further, Eq. 3.1 always yields good fits for these same g-factors, also when applied to data in the range 0 T to 3 T. In our earlier work we identified the contribution with $|g_1| \approx 0.36$ as a population in the 2DEG layer, and the contribution with $|g_2| \approx 0.43$ as a population in a bulk GaAs layer [19]. The slow growth during delays till ∼100 ps (as compared to mono-exponential decay for a single population) of signals (at 0 T) and signal envelopes also originates from having a superposition of two contributions. It occurs because the amplitudes A_i always have opposite sign (for ϕ_i around zero) [19].

SDA is apparent in the zero-field Kerr signals in Fig. 3.2(a) from wires oriented along the [110], [-110], [100], and [010] (and for reference from unpatterned area). The decay of signals during delays $t > 100$ ps clearly depends on the wire orientation. The loss of Kerr signal is fastest for [-110] oriented wires (only slightly slower than for unpatterned area). Kerr signal decay is slowest for [110] oriented wires, and results for wires in [100] and [010] directions are in between these extreme cases and nearly identical. The inset of Fig. 3.2(a) shows that the time scale for slow signal growth for $t < 100$ ps has a similar dependence on wire orientation, with again the slowest time scale for the [110] direction. For the Kerr signals measured in the range 1 T to 7 T in Fig. 3.3(a), all traces have envelopes with slow growth for $t < 100$ ps, and decaying envelopes for $t > 100$ ps as the zero-field signals. At 1 T, the corresponding time scales are again clearly longest for [110] wires and shortest for [-110] wires but the differences degrade for $B > 1$ T. We only present signals for the extreme cases [-110] and [110], results for [100] and [010] wires show intermediate behavior.

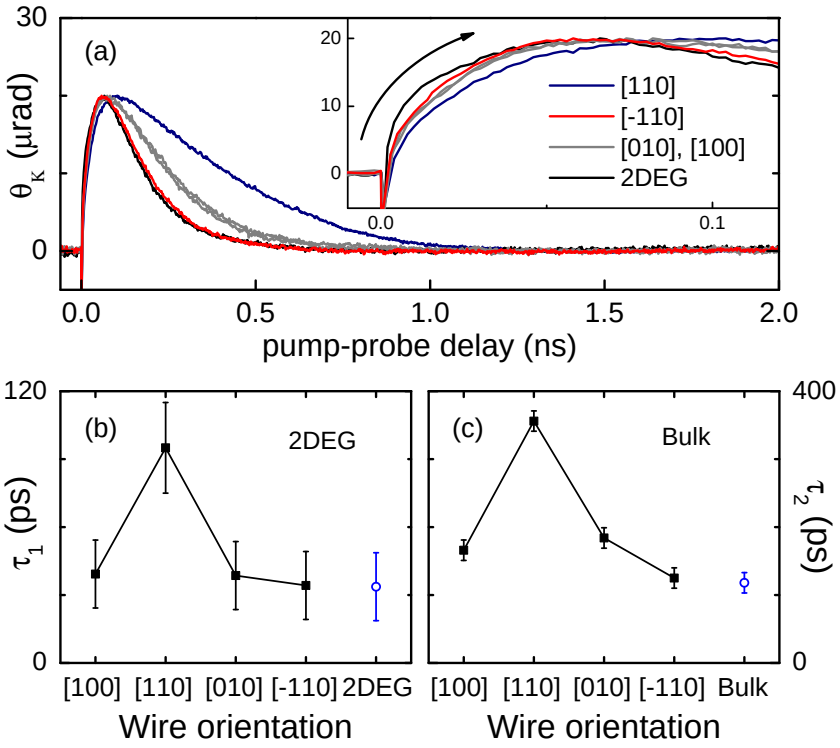

Figure 3.2: Spin-dephasing anisotropy at zero external magnetic field. (a) Kerr rotation as a function of pump-probe delay for the unpatterned area and wires in [-110], [110], [100], and [010] directions (order along arrow in traces and legend match). The inset shows the Kerr response at short delays to highlight the slow growth in all traces. [(b) and (c)] Spin-dephasing times for both the 2DEG (τ_1) and bulk (τ_2) spin populations.

Fitting these results with Eq. (3.1) yields traces which very closely match the experimental traces (therefore not shown). Signals from $B \geq 1$ T give results for τ_i for both the 2DEG ($|g_1| \approx 0.36$) and bulk ($|g_2| \approx 0.43$) contributions to the signals [Figs. 3.3(b) and 3.3(c)]. This identifies that the time scale for slow growth ($t < 100$ ps) is dominated by dephasing of the 2DEG population, while the later decay of signals ($t > 100$ ps) is dominated by dephasing of a bulk population. The behavior for $B = 0$ T [Figs. 3.2(b) and 3.2(c)] is interpreted in the same way from extrapolating down the trends in τ_i for $B > 0$ T. This identification of populations based on g factors is consistent with reported values for dephasing times in high-mobility 2DEGs [∼50 ps due to rapid D'yakonov-Perel' (DP) dephasing [3, 21, 22]] and intrinsic GaAs layers [∼300 ps [17]].

The results in Figs. 3.2(b) and 3.3(b) give clear evidence for SDA for the 2DEG

population, with qualitative agreement with predicted behavior [15, 23]. These predictions were based on the assumption that Rashba and linear Dresselhaus SOI terms dominate. Expressed as k-vector-dependent effective fields these are $\vec{B}_R = C_R(\hat{x}k_y - \hat{y}k_x)$ and $\vec{B}_{D1} = C_{D1}(-\hat{x}k_x + \hat{y}k_y)$, respectively, with typical magnitudes of about 2 T for heterojunction 2DEGs [3]. A summary of the numerical approach is given below for the bulk population. The dependence of 2DEG dephasing on wire orientation is here less strong than expected for exact cancellation for $C_{D1} = C_R$ [15, 4]. Instead, it is consistent with simulations for $|C_{D1}+C_R|/|C_{D1}-C_R| \approx 3$

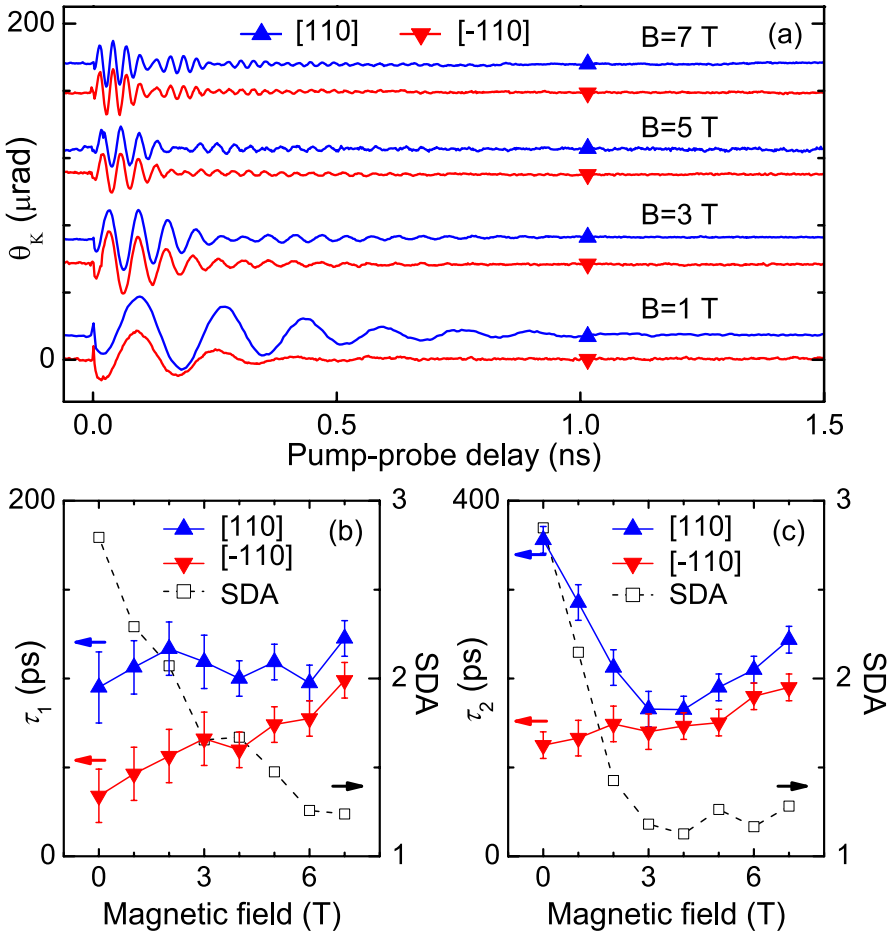

Figure 3.3: Evolution of spin-dephasing anisotropy (SDA) in transverse magnetic fields up to $B = 7$ T. (a) Kerr signals as a function of pump-probe delay from [110] and [-110] oriented wires (traces offset for clarity). [(b) and (c)] Corresponding spin dephasing times τ_i as a function of B, for (b) 2DEG and (c) bulk electrons. These plots also present SDA quantified as $\tau_{i,[110]}/\tau_{i,[-110]}$.

and C_{D1} and C_R as reported values [3]. We cannot make more detailed statements about C_{D1} and C_R values since we analyzed that this should account for the influence of the cubic Dresselhaus SOI, momentum relaxation, and electron-hole recombination on the observed Kerr signals. The dependence of SDA on B is discussed below.

The SDA observed for spins in a bulk layer in Figs. 3.2(c) and 3.3(c) was an unexpected result since SDA was until now only considered for 2D electron systems. Apparently, our samples also contain quasi-1D ensembles with bulk characteristics that have anisotropy for SOI. Such ensembles must indeed be present because band bending is significant up to $\sim$2 μm below the wafer surface. Consequently, the lifting of the conduction band below etched areas also induces confining potentials along the wires at the depth of the superlattice (which also drives a rapid drift of photoelectrons from etched to unetched areas, such that the bulk contribution to signals is mainly from unetched regions). In addition, below the wires (areas not etched) at the depth of the superlattice there is still a weak slope in the conduction band [Fig. 3.1(c)]. A Rashba SOI should be effective here that only depends on the x and y component of a k vector as for the 2DEG case. Here the Rashba parameter $C_R \propto \langle dV/dz \rangle$ still has a substantial value [24] due to the slope of the conduction band (V is potential of the bottom of conduction band and z is growth direction). This results in anisotropic SOI [analogs to Fig. 3.1(a)] when this Rashba term has a similar magnitude as the Dresselhaus SOI for bulk [23].

We therefore conjecture that the observed SDA for a bulk population is due to electrons *around* (*i.e.*, not inside [19]) the superlattice. The Kerr reflection from the superlattice will probe the spin imbalance in its vicinity. Most likely, this population is located in the accumulation layer [Fig. 3.1(c)] since the thickness of this layer is sufficient for absorbing most of the energy from our laser pulses. The separation into two distinct spin populations can then only be explained if we assume the surprisingly low mobility for photo-electrons along the growth direction that was recently reported [25]. We can therefore not fully rule out scenarios where the bulk response is dominated by electrons at the substrate side of the superlattice, given that these low mobility values are not yet fully understood [19].

3.4 Summary of numerical simulations

To investigate the above scenario, we use a simple model and Monte Carlo simulations as for 2DEG-based wires [15]. The short summary presented here is based on the work presented in *Chapter 4* and *Chapter 5*. We model a wire of bulk material by assuming a randomly moving electron ensemble with a three-dimensional k vector distribution that is confined to a rectangular elongated box with short sides of 1 μm. The electrons are scattering on the edge of the box and on impurities (mean-free path from impurities alone set at 1 μm, *i.e.*, a quasiballistic electron ensemble). The (quasi-)Fermi level is derived from the estimated photo-electron density around the superlattice ($\sim 3 \cdot 10^{21}$ m^{-3}). Spins are precessing around the sum of anisotropic spin-orbit fields and the external field. We assume the electron spins experience only the bulk Dresselhaus SOI Ref.([2]), and the mentioned Rashba SOI. Dephasing is again purely due to the DP mechanism. Such numerics indeed produces dephasing times similar to the observed values. Also, it shows SDA as a function of wire orientation with the slowest dephasing for wires along [110] and with the ratio between τ_2 for [110] and [-110] wires close to 3 for $B = 0$ T.

3.5 Effect of external magnetic field on spin dephasing anisotropy

As an extra point we discuss the magnetic field dependence of SDA for the 2DEG and bulk populations. For both, the SDA (taken as the ratio between dephasing times for [110] and [-110] wires, see Figs. 3.3(b) and 3.3(c)) is most apparent at zero external field, and degrades with increasing field. Our type of SDA only occurs in quasi-1D systems, *i.e.*, when the width of the wires is less than the spin precession length L_{sp} [15]. Alternatively, it can degrade when an external field starts to dominate over anisotropic spin-orbit fields [Fig. 3.1(a)]. The degradation of SDA of the bulk population is consistent with both explanations. The external field drives L_{sp} below $\sim$1 μm for $B \approx 4$ T (using again the estimated density of photo-electrons around the superlattice) but we also estimate [3] that the external field dominates over spin-orbit fields above $B \approx 0.3$ T. For the 2DEG a much stronger field is needed for driving $L_{sp} \lesssim 1$ μm, but the external field dominates over spin-orbit fields for $B > 4$ T [3]. We repeated all measurements with the external field in [-110] direction. We observed small shifts ($\sim$ 10%) in the dephasing times, but the B dependence of SDA was at nearly the same

level. We interpret this as follows. Having only partial cancellation of SOI (not the pure case $C_{D1} = C_R$) gives anisotropy for SOI with fields varying both in magnitude and direction. This still gives SDA, but it can be lifted by adding an external field that is stronger than the spin-orbit fields, and there is then little dependence on the direction of the field. Our Monte-Carlo simulations confirm this behavior, and give SDA values that degrade from ∼3 at $B = 0$ T to ∼2 at 7 T.

3.6 Effect of temperature and pump power on spin dephasing anisotropy

The dependence on temperature can provide more insights in the spin dephasing anisotropy, since the spin dephasing time of bulk and 2DEG changes differently with temperature [17].

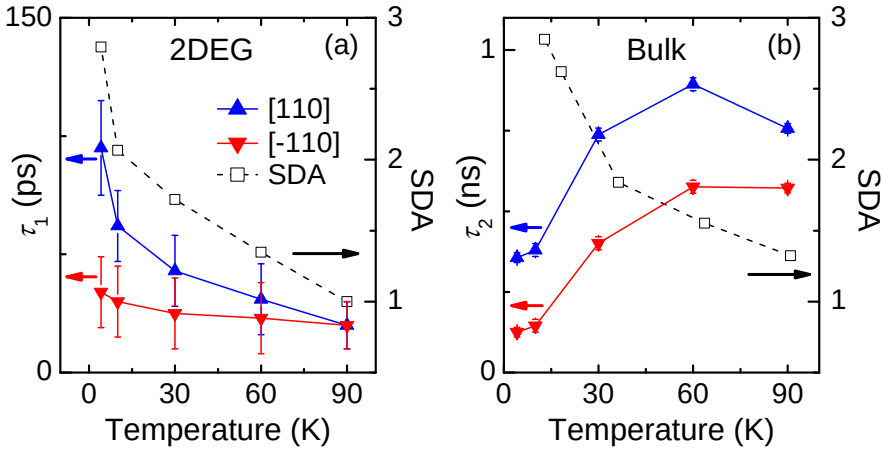

Figure 3.4: Effect of temperature on spin-dephasing anisotropy (SDA). [(a) and (b)] The spin dephasing times τ_i as a function of T, for (a) 2DEG and (b) bulk electrons. These plots also present SDA quantified as $\tau_{i,[110]}/\tau_{i,[-110]}$.

The measurements were performed at a few different temperatures for the case zero external magnetic field. The spin dephasing anisotropy is decaying with increasing temperature for both: 2DEG and bulk. However, 2DEG and bulk show an opposite trend for the actual values of the spin dephasing times. While the spin dephasing time of 2DEG is rapidly decreasing with temperature, the bulk exhibits the opposite behavior. This can be explained by the effective

change in spin precession length due to temperature dependence of the electron mobility.

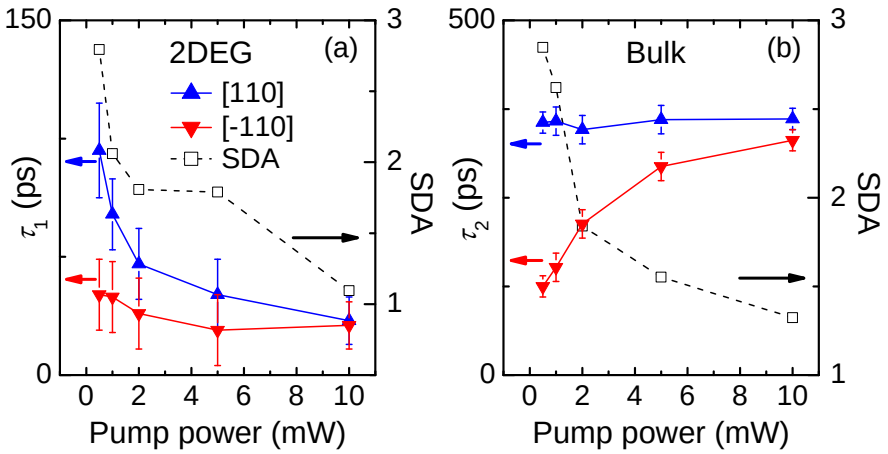

Figure 3.5: Effect of excited electron density tuned by means of the pump power. [(a) and (b)] The spin dephasing times τ_i as a function of pump power, for (a) 2DEG and (b) bulk electrons. These plots also present SDA quantified as $\tau_{i,[110]}/\tau_{i,[-110]}$.

Increasing the number of photo-excited (spin polarized) carriers also strongly affects the spin dephasing anisotropy. For low pump powers (where the number of photo-excited electrons is comparable to the number of electrons already present in the 2DEG) the previous picture of the spin dephasing anisotropy mechanism holds. For higher excitation densities (above roughly 2 mW of pump power) the number of photo excited carriers exceeds the number of native electrons in the system. This generates a strong self-screening effect, which reduces the mobility in a transient manner (due to electron-hole recombination at a timescale of about 300 ps). Having such a process in the sample strongly affects the dynamics of the ensemble of spin, which can no longer be considered as a ballistic electron ensemble in a wire with fixed transport properties over the measurement period. Strong pumping also increases the effective temperature in the system and this contributes to the reduction of the SDA when increasing the pump powers.

As a conclusion, we note that the results of the study of the temperature dependence and the pump-power dependence are consistent with our interpretation of having an SDA effect for both a 2DEG and a bulk population in the system.

3.7 Conclusions

In conclusion, our results confirm that confining electron ensembles in quasi-1D wires in [110] direction can yield suppressed spin dephasing. The results agree with predictions based on anisotropy for SOI. Further studies with tuning of SOI by a gate gives access to better cancellation of Rashba and Dresselhaus SOI, and can explore the ultimate limit of suppressing dephasing in wires [4, 15]. Such gate control can also yield spin-transistor functionality [1] by associating *on* and *off* with strong or little dephasing of spin signals. Our results also establish that using SDA for suppressing dephasing is not restricted to quantum-well electron ensembles. It is also applicable to quasi-1D ensembles in bulk-like layers where the conduction band has a slope. Our results thus open the path to investigating the mentioned spin-transistor functionality for bulk semiconductor channels [26].

We thank R. Winkler and A. Rudavskyi for discussions, and the Dutch NWO and NanoNed, and the German programs DFG-SFB 491, DFG-SPP 1285 and BMBF nanoQUIT for financial support.

References

[1] D. D. Awschalom and N. Samarth, Physics **2**, 50 (2009).

[2] For a review see R. H. Silsbee, J. Phys. Condens. Matter **16**, R179 (2004).

[3] J. B. Miller, D. M. Zumbuhl, C. M. Marcus, Y. B. Lyanda-Geller, D. Goldhaber-Gordon, K. Campman, and A. C. Gossard, Phys. Rev. Lett. **90**, 076807 (2003).

[4] J. D. Koralek, C. P. Weber, J. Orenstein, B. A. Bernevig, S. C. Zhang, S. Mack, and D. Awschalom, Nature (London) **458**, 610 (2009).

[5] N. S. Averkiev and L. E. Golub, Phys. Rev. B **60**, 15582 (1999).

[6] J. Schliemann, J. C. Egues, and D. Loss, Phys. Rev. Lett. **90**, 146801 (2003).

[7] B. A. Bernevig, J. Orenstein, and S.-C. Zhang, Phys. Rev. Lett. **97**, 236601 (2006).

[8] J. L. Cheng, M. W. Wu, and I. C. da CunhaLima, Phys. Rev. B **75**, 205328 (2007).

[9] M. Duckheim and D. Loss, Phys. Rev. B **75**, 201305(R) (2007).

[10] N. S. Averkiev, L. E. Golub, A. S. Gurevich, V. P. Evtikhiev, V. P. Kochereshko, A. V. Platonov, A. S. Shkolnik, and Y. P. Efimov, Phys. Rev. B **74**, 033305 (2006).

[11] T. Korn, D. Stich, R. Schulz, D. Schuh, W. Wegscheider, and C. Schller, Physica E **40**, 1542 (2008).

[12] A. W. Holleitner, V. Sih, R. C. Myers, A. C. Gossard, and D. D. Awschalom, Phys. Rev. Lett. **97**, 036805 (2006).

[13] Y. Kunihashi, M. Kohda, and J. Nitta, Phys. Rev. Lett. **102**, 226601 (2009).

[14] S. M. Frolov, S. Lscher, W. Yu, Y. Ren, J. A. Folk, and W. Wegscheider, Nature (Londen) **458**, 868 (2009).

[15] J. Liu, T. Last, E. J. Koop, S. Denega, B. J. van Wees, and C. H. van der Wal, J. Supercond. Novel. Magn. **23**, 11 (2010).

[16] Y. Kunihashi, M. Kohda, and J. Nitta, Physics Procedia **3**, 1255 (2010).

[17] J. M. Kikkawa and D. D. Awschalom, Phys. Rev. Lett. **80**, 4313 (1998).

[18] We checked that grating behavior of the arrays did not influence Kerr signals, by rotating the polarization planes of the pump and probe beam around their axes.

[19] P. J. Rizo, A. Pugzlys, A. Slachter, S. Z. Denega, D. Reuter, A. D. Wieck, P. H. M. van Loosdrecht, and C. H. van der Wal, New J. Phys. **12**, 113040 (2010).

[20] We observe that using phases ϕ_i as free parameters is needed for obtaining good fits. We only use data from delays $t > 5$ ps, since holes contribute to the Kerr signals up to $t \approx 5$ ps. For $t < 5$ ps there is also rapid relaxation of electron kinetic energy, which can contribute to apparent phase offsets for $t > 5$ ps [19].

[21] M. J. Snelling, G. P. Flinn, A. S. Plaut, R. T. Harley, A. C. Tropper, R. Eccleston, and C. C. Phillips, Phys. Rev. B **44**, 11345 (1991).

[22] D. Stich, J. Zhou, T. Korn, R. Schulz, D. Schuh, W. Wegscheider, M. W. Wu, and C. Schuller, Phys. Rev. Lett. **98**, 176401 (2007).

[23] We analyzed that SOI due to possible presence of wire-induced strain cannot explain the observed SDA.

[24] As compared to the 2DEG case, where the slope in V for the GaAs layer is compensated by the steep increase in V at the heterojunction, since 2DEG states penetrate the AlGaAs layer (Fig. 3.1(c)).

[25] G. Salis and S. F. Alvarado, Phys. Rev. Lett. **96**, 177401 (2006).

[26] S. P. Dash, S. Sharma, R. S. Patel, M. P. de Jong, and R. Jansen, Nature **462**, 491 (2009).